Vertical coupling of long-range surface plasmon polaritons

Cite as: Appl. Phys. Lett. **88**, 011110 (2006); https://doi.org/10.1063/1.2159558
Submitted: 10 May 2005 • Accepted: 09 November 2005 • Published Online: 04 January 2006

Hyong Sik Won, Ki Cheol Kim, Seok Ho Song, et al.

Vertical coupling of long-range surface plasmon polaritons

Hyong Sik Won, Ki Cheol Kim, Seok Ho Song,[a] Cha-Hwan Oh, and Pill Soo Kim
Department of Physics, Hanyang University, Seoul 133-791, Korea

Suntak Park
Electronics and Telecommunications Research Institute, Dajeon 305-350, Korea

Sang In Kim
Department of Electrical Engineering, Ajou University, Suwon 443-749, Korea

(Received 10 May 2005; accepted 9 November 2005; published online 4 January 2006)

We evaluated and demonstrated strong vertical-coupling characteristics of vertical directional couplers based on long-range surface plasmon polaritons (LRSPPs) at 1.55 μm wavelength. Fundamental even and odd modes supported by LRSPP metal-stripe waveguides compete more strongly on vertical coupling structures than on lateral coupling structures, possibly leading to less power consumption for switching and to compactness in device length and width. LRSPP-based vertically coupled routing of signals can also be a powerful means of developing three-dimensional photonic integrated circuits and optical printed circuit boards. © *2006 American Institute of Physics*. [DOI: 10.1063/1.2159558]

The rapid development of information technology demands highly integrated optical circuits. The miniaturization of optical components is one way to increase the density of optical integrated circuits. Miniaturization may be accomplished by adopting photonic crystal structures,[1] high-refractive-index dielectrics,[2] metal-dielectric hybrid waveguides,[3] and pure metal wires embedded in dielectrics.[4] In particular, metal wires which support long-range surface plasmon polaritons (LRSPP) are studied intensively because such a stripe can carry electrical signals along with the LRSPP modes.[5] LRSPP-based thermo-optic devices[6] of Mach-Zender interferometric modulators and directional couplers demonstrated recently are good examples of electrically controlled LRSPP components.

Interferometric modulators exhibit considerably lower driving power because the control electrode is positioned at precisely the maximum amplitude of the LRSPP modes, while the directional-coupler switches require power supplies an order of magnitude larger than those of interferometric modulators. It appears that mode-switching *lateral* directional couplers (LDCs) with two side-by-side (coplanar) metal stripes on the same plane may be an inefficient way to heat the thermo-optic materials surrounding the metal stripes, because the cross section of the mode-coupling region between the two coplanar stripes has a typical thickness of only ~10 nm. Therefore, a *vertical* directional coupler (VDC), which is composed of two metal stripes stacked layer upon layer, might be a more promising way to increase the width of the cross section up to at least several micrometers and consequently reduce power requirements. In general, vertically coupled multilayer structures with alternative pairs of metal-dielectric films[7] can be a powerful means of developing three-dimensional (3-D), multilayered photonic integrated circuits (PICs).[8] By transitioning to multilayer interconnects with vertically coupled metal stripes, LRSPP-based signal routing will be very advantageous for more compact and more functional photonic integrated circuits and optical printed circuit boards.[9]

Here, we report the characteristics of the vertical coupling of LRSPPs in VDCs operating at 1.55 μm wavelength. At a given vertical separation, (4 μm between two parallel metal stripes of VDCs) we demonstrated strong mode-coupling behavior between two fundamental modes with even (symmetric) and odd (antisymmetric) field distributions. The metal waveguide considered here consists of 20 nm thick, 5 μm wide gold stripes embedded in a homogeneous dielectric. Evaluation of propagation constants and field profiles of the coupled modes was performed by using the method of lines.[10] We found that coupling length (L_c) of the VDCs, which is defined by the minimum length required for transferring completely the optical power of one channel to the other, was at least three times shorter than that of LDCs under the same stripe separation. Minimum separation between two stripes was limited by odd modes in both coupler types since the effective indices of the odd modes rapidly approach the index of the surrounding dielectric when the vertical separation is reduced.

Figure 1(a) shows a schematic layout and 1(b) shows a microscope image of the VDCs fabricated in the experiment. A polarization maintaining single-mode fiber carrying an optical signal with TM polarized, 1.55 μm wavelength is end-

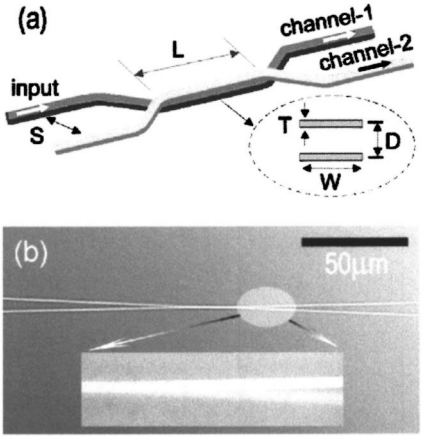

FIG. 1. (a) Schematic diagram of a VDC with two vertically stacked metal stripes. (b) An optical microscope image of the fabricated VDCs. The inset shows a magnification of the stacked metal stripes.

[a]Electronic mail: shsong@hanyang.ac.kr

fired while coupled to one (input) of the two metal stripes, and the input signal is transmitted to either one or both of the output ports, channel 1 and channel 2, according to the interaction length (L) of the parallel stripe region depicted in Fig. 1(a). Sixteen VDCs with different lengths (L), from 200 μm to 500 μm in increments of 20 μm, were fabricated on the same Si wafer, while the overall device length was maintained at 9 mm. The thickness (T) and width (W) of the metal stripes were 20 nm and 5.0 μm, respectively, and the vertical separation distance (D) between the upper and lower stripes was 4.0 μm. The lateral spacing (S) of the input and output ports was fixed at 200 μm, and the split angle between two stripes before they overlap was 1.9°. A magnified image (×1000) presented in the inset of Fig. 1(b) clearly shows the split angle of the two vertically stacked metal stripes, by focusing the microscope on the upper stripe showing sharp outlines. The fabrication process is as follows. First, the under cladding, a 12 μm thick layer of fluorinated acrylate photopolymer resin (ZPU12-470, ChemOptics Inc.), was spin coated onto a silicon wafer. The coated resin was then cured by UV (300 W, 8 min) and thermal (170 °C, 30 min) exposures in sequence. The refractive index of the photopolymer resin was designed to be 1.470 at 1.55 μm after the curing process. After stripe patterning of a photoresist layer (AZ 5206, Hoechst) and thermal evaporation of an additional adhesion layer (1 nm thick, Cr), the lower gold stripe with a thickness of 20 nm and a width of 5.0 μm was formed by conventional liftoff photolithography. The lower stripe was then covered again with the spin-coated, 4.0 μm thick middle cladding layer (ZPU12-470). The same process was repeated for the upper gold stripe and the 12 μm thick upper cladding layer. Vertical positioning of the two overlayered gold stripes was done with a commercial mask aligner.

In the theoretical evaluation of the field profiles and propagation constants of the coupled modes supported by the VDCs, we used material parameters including the PR ($n=1.6$) and Cr ($\varepsilon=-5.2+40i$) layers, and the 20 nm thick gold layer ($\varepsilon=-118+11.58i$). The evaluation results are shown in Fig. 2. Electric field amplitudes $|\boldsymbol{E}|$ of two fundamental LRSPP modes (even mode and odd mode) supported by the two vertically coupled metal stripes are presented in Fig. 2(a). The even mode at the left of Fig. 2(a) has a symmetrically coupled profile between two ss_b^o modes,[11] which are respectively supported by each of the 20-nm-thick metal stripes before coupling, while the odd mode at the right has an antisymmetrically coupled profile. (Note that the direction of the electric field is the same at all positions in the even mode, but opposite in upper and lower halves of the odd mode.) The odd mode exhibits a dip ($|\boldsymbol{E}|=0$) at the middle of the vertically coupled region and spreads widely toward the upper and lower cladding layers. The even mode is more confined to the middle cladding layer that is sandwiched between the two metal stripes, resulting in increased propagation loss for the even mode as D decreases. Figure 2(b) shows the attenuation constants (β_i/k_0) of the two LRSPP modes when D varies from 0 μm to 25 μm, and the effective indices are shown ($n_{\text{eff}}=\beta_r/k_o$) in the inset. Here, β_r and β_i are real and imaginary components, respectively, of the propagation constants of LRSPP modes, and k_o is the vacuum wave number. When D is reduced, the even mode exhibits a rapid increase in loss represented by the attenuation constants, after crossing at $D=7.3$ μm with the odd mode, but the attenuation constant of the odd mode decreases down under 10^{-4} before it becomes a leaky mode at the cutoff distance of 3.8 μm. We chose $D=4.0$ μm in the experiment for deriving a stronger coupling strength between LRSPPs excited at the two metal stripes, but the extinction ratio of the VDCs must be maximized when D approaches the crossing point of 7.3 μm. For large separation distances, D of the even and odd modes have the same effective index of 1.472, while for D smaller than a certain threshold near 15 μm, the coupling strength is strong enough to split the effective index toward two limit values, 1.479 when $D=0$ μm for the even mode and 1.470 when $D=3.8$ μm for the odd mode.

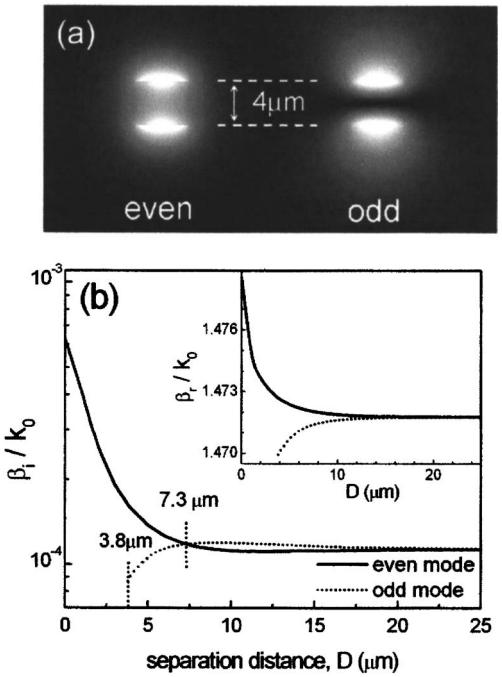

FIG. 2. (a) Electric-field distributions of the even and odd modes supported by two parallel, vertically coupled metal stripes. The brighter is larger in field amplitude. (b) Attenuation constants (β_i/k_o) of the two modes. The inset shows effective indices (β_r/k_o).

Figure 3(a) shows the normalized output powers measured at channel 1 (squares) and channel 2 (open circles) for the 16 VDCs fabricated with different interaction lengths L from 200 to 500 μm. The measured powers in both channels are well fitted to the solid curves of $\sin^2(\kappa L)$, where $\kappa=k_o\delta n_{\text{eff}}$ and δn_{eff} is the effective index difference of the even and odd modes.[12] Therefore, we can determine the coupling length L_c of the VDCs as follows: $L_c=\pi/\kappa=298$ μm since $\delta n_{\text{eff}}=0.0026$ for $D=4$ μm. This coupling length can also be confirmed by the IR-camera images of output signals, as shown in Fig. 3(b). When $L=410$ μm, at the right-hand side of the bottom image the channel 2 output is almost eliminated with an extinction ratio of 28 dB between two channel outputs, while the outputs for $L=260$ μm exhibit a small difference in power, as shown in the top image. Some noise of stray lights guided by the dielectric cladding may occur between the desired output spots; thus, it is very important to maintain index homogeneity of the dielectric surrounding the metal stripes.[13]

To compare the device characteristics of VDCs and LDCs in more detail, we examined two gold stripes, each 20 nm thick and 5 μm wide, which were embedded in the

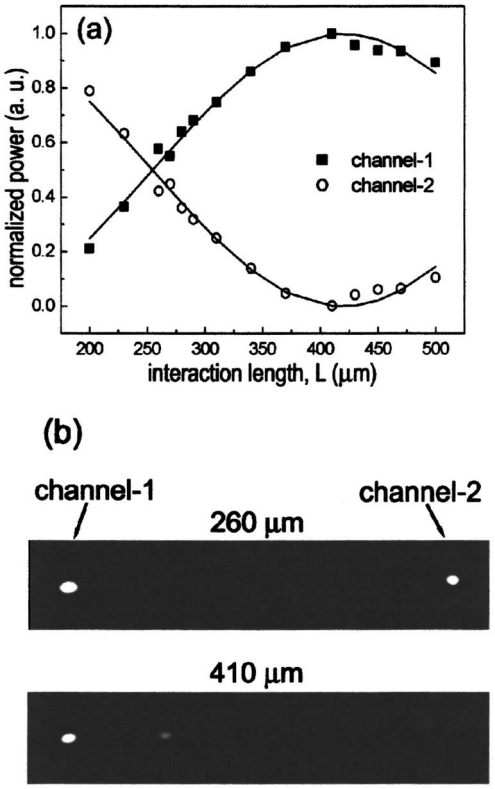

FIG. 3. Measured channel outputs of the VDCs with various interaction lengths. (a) Normalized optical powers of the two output channels. Solid curves are $\sin^2(\kappa L)$ functions fitted to the measured data (small squares and circles). (b) IR images of the channel outputs when $L=260$ μm (top) and $L=410$ μm (bottom).

photopolymer dielectric without the Cr layers, which were used in the first experiment. The LDCs considered here have a structure similar to the VDCs shown in Fig. 1(a), but the two metal stripes were placed on the same plane with separation distances D defined by the edge-to-edge spacing difference. Figure 4 shows attenuation constants (β_i/k_o) of the even and odd modes excited at VDCs (solid curves) and LDCs (dashed curves) when D varies from 0 μm to 30 μm. Without use of the Cr layers, the VDCs exhibited attenuation constants an order of magnitude lower than those with Cr layers, as presented in Fig. 2(b), and the critical distances of mode cutoff (7.4 μm) and mode crossing (9.7 μm) increase considerably. The mode cutoff (3 μm) and mode crossing (6.8 μm) in LDCs occur when metal stripes are closer together, which means that LRSPPs excited at both of the metal stripes experience much stronger interaction in a vertical configuration. This strong LRSPP-coupling effect in VDCs can also be confirmed by checking the coupling lengths L_c of VDCs (solid curve) and LDCs (dashed curve), which are depicted in the inset of Fig. 4. At a given D above 7.4 μm, the VDC's L_c is about three times shorter than the LDC's. Even at their mode-crossing distances of 9.7 μm in VDC and 6.8 μm in LDC, which guarantee their maximum extinction ratios, the VDC is superior in device compactness since $L_c=1.6$ mm for the VDC and $L_c=2.3$ mm for the LDC. One may expect an increase in device cost caused by multilayer processing in VDC fabrication; nevertheless, we believe that LRSPP-based vertical waveguide structures have some significant advantages. If we implement a VDC switch by applying electrical power to the metal stripes embedded

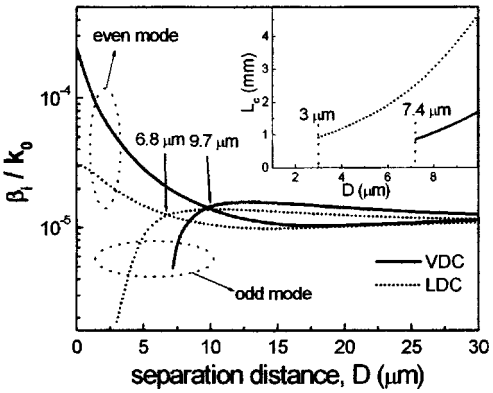

FIG. 4. Comparison on attenuation constants β_i/k_o of VDCs (solid curves) and LDCs (dashed curves). The inset shows coupling lengths L_c for completely transferring output power from one channel to the other.

in a dielectric with thermo-optic or electro-optic effects, the VDC switch requires less switching power due to its strong mode-coupling interaction. In addition the use of optical Kerr media sandwiched in between the vertically stacked metal stripes may allow for the realization of nonlinear LRSPP devices, which can be driven by lower optical power. Some periodic elements, such as dielectric gratings[14] could be properly sandwiched at the gap between metal waveguides for enriching the device functionality of VDCs.

In conclusion, we evaluated and demonstrated strong vertical-coupling effects of vertical directional couplers based on LRSPP waveguides. The fundamental even and odd modes supported by two metal stripes compete more strongly in VDC structures than in LDCs, leading to possibly less power consumption for switching in VDCs. In addition, the leap to multilayer interconnects with metal stripes enables us to imagine *hybrid* 3-D PICs in which electrical and optical signals are delivered through a common metal wire.

This work was supported by Grant No. R01-2005-000-10276-0(2005) from the Basic Research Program of the Korea Science & Engineering Foundation.

[1] S. Noda and T. Baba, *Roadmap on Photonic Crystals* (Kluwer Academic, Boston, 2003).
[2] B. E. Little, J. S. Foresi, G. Steinmeyer, E. R. Thoen, S. T. Chu, H. A. Haus, E. P. Ippen, L. C. Kimerling, and W. Greene, IEEE Photonics Technol. Lett. **10**, 549 (1998).
[3] M. Hochberg, T. Baehr-Jones, C. Walker, and A. Scherer, Opt. Express **12**, 5481 (2004).
[4] J. Weeber, A. Dereux, and C. Girard, Phys. Rev. B **60**, 9061 (1999).
[5] R. Charbonneau, N. Lahoud, G. Mattiussi, and P. Berini, Opt. Express **13**, 977 (2005).
[6] T. Nikolajsen, K. Leosson, and S. I. Bozhevolnyi, Appl. Phys. Lett. **85**, 5833 (2004).
[7] D. Sarid, Phys. Rev. Lett. **47**, 1927 (1981).
[8] M. Raburn, B. Liu, K. Rauscher, Y. Okuno, N. Dagli, and J. E. Bowers, IEEE J. Sel. Top. Quantum Electron. **8**, 935 (2002).
[9] B. Witlmann, S. Lehmacher, S. Kopecz, and A. Neyer, Int. J. Electron. Commun. **55**, 319 (2001).
[10] P. Berini and K. Wu, IEEE Trans. Microwave Theory Tech. **44**, 749 (1996).
[11] P. Berini, Phys. Rev. B **61**, 10484 (2000).
[12] K. Okamoto, *Fundamentals of Optical Waveguides* (Academic, New York, 2000).
[13] G. Mattiussi, N. Lahoud, R. Charbonneau, and P. Berini, Proc. SPIE **5720**, 173 (2005).
[14] S. Park, G. Lee, S. H. Song, C.-H. Oh, and P.-S. Kim, Opt. Lett. **28**, 1870 (2003).